Finite-temperature corrections to the time-domain equations of motion for perpendicular propagation in nonuniform magnetized plasmas

W. Tierens[1, a)] and D. De Zutter[1, b)]
Ghent University, Department of Information Technology, Sint-Pietersnieuwstraat 41, Ghent, Belgium

(Dated: 1 October 2012)

In this paper we extend the new techniques of[1], to include finite Larmor radius effects up to second order in the Larmor radius. We limit ourselves to the case of propagation perpendicular to the background magnetic field $\vec{B}_0$. We show that our time-domain technique is able to produce the lowest-order Bernstein wave (a wave believed to be useful for heating fusion devices[2]). The discrete equations retain many of the favourable properties described in[1], i.e. unconditional stability and a straightforward relation between the second-order accurate continuous dispersion relation and the dispersion relation of the discretized problem. The theory is illustrated by a place-independent and a place-dependent temperature numerical example.

PACS numbers: 52.30,52.50
Keywords: Cold plasma, Warm plasma, finite Larmor radius, time domain

I. INTRODUCTION

Finite-temperature effects are usually included in models of wave propagation in magnetized plasmas by adding corrections to the wave equation, e.g.[3,4] and many others.

Attempts to include finite-temperature / finite-Larmor-radius effects directly in the time-domain equations of motion are far less common. Young[5] attemps to use an additional pressure term to include "warm" behaviour. The issue is also briefly discussed by Smithe[6].

In this paper, we will derive finite-Larmor-radius corrections to the well-known cold plasma equations of motion[7]

$$\frac{\partial}{\partial t}\vec{J}_s = \epsilon_0\omega_s^2\vec{E} + \vec{\Omega}_s \times \vec{J}_s \tag{1}$$

for perpendicular propagation ($\vec{k} \perp \vec{B}_0$). By carefully choosing the approximations, we obtain a set of equations which remains unconditionally stable even outside of the approximations' range of physical validity. We then discretize these equations using the time-domain techniques described in[1].

This paper is structured as follows: in section II, we describe a rather general technique for obtaining time-domain differential equations to model a material given a frequency-domain dielectric tensor. In section III, we apply this technique to derive equations of motion for warm plasma for perpendicular propagation. In section IV, we construct the equations for non-uniform plasma. In section V, we discretize these equations of motion in an unconditionally stable way. We give two numerical examples in section VI, a first one for uniform plasma and a second one for nonuniform plasma. Finally we present the conclusions in section VII.

a)Electronic mail: wouter.tierens@ugent.be
b)Electronic mail: daniel.dezutter@ugent.be

II. OBTAINING CONSTITUTIVE EQUATIONS FOR PLASMAS

Deriving constitutive equations from frequency-domain dielectric tensors is discussed, in very general terms, in[8]. Here we present a slight generalization of that technique.

Maxwell's 'macroscopic' equations are

$$\vec{\nabla} \times \vec{E} = -\frac{\partial \vec{B}}{\partial t} \tag{2}$$

$$\frac{1}{\mu_0}\vec{\nabla} \times \vec{B} = \frac{\partial \vec{D}}{\partial t} \tag{3}$$

$$\vec{D} = \epsilon_0\epsilon_r \cdot \vec{E} \tag{4}$$

where ϵ_r is a 3×3 tensor.

In plasmas we generally have

$$\epsilon_r = 1 + \sum_{\text{specie } s} \epsilon_{r,s} \tag{5}$$

The 'microscopic' equivalent of (3) is

$$\frac{1}{\mu_0}\vec{\nabla} \times \vec{B} = \epsilon_0\frac{\partial \vec{E}}{\partial t} + \sum_{\text{specie } s} \vec{J}_s \tag{6}$$

hence

$$\epsilon_0\frac{\partial \vec{E}}{\partial t} + \sum_{\text{specie } s} \vec{J}_s = \frac{\partial \vec{D}}{\partial t} = \epsilon_0\left(1 + \sum_{\text{specie } s} \epsilon_{r,s}\right) \cdot \frac{\partial \vec{E}}{\partial t} \tag{7}$$

$$\sum_{\text{specie } s} \vec{J}_s = \sum_{\text{specie } s} \epsilon_0\epsilon_{r,s} \cdot \frac{\partial \vec{E}}{\partial t} \tag{8}$$

If currents in a material are given by

$$\vec{J}_s = \epsilon_0\epsilon_{r,s} \cdot \frac{\partial \vec{E}}{\partial t} \tag{9}$$

then (8) holds and the dielectric tensor is given by (5).

III. CONSTITUTIVE EQUATIONS FOR PERPENDICULAR PROPAGATION $k_\parallel = 0$ IN UNIFORM WARM PLASMA

The background magnetic field $\vec{B}_0$ is assumed to be along the z-direction, and the propagation direction along the x-direction. Using these assumptions, the hot plasma dielectric tensor is derived in[9] as an infinite sum (summation index n), of which a finite-order approximation will only need to retain finitely-many terms. As in the cold plasma case, for perpendicular propagation, there are two independent solutions, with the electric field parallel resp. perpendicular to $\vec{B}_0$. We will consider the $\vec{E} \perp \vec{B}_0$ case here. Hence, we will need the x, y part of the hot plasma dielectric tensor in the $k_\parallel = 0$ case.

We want to construct constitutive equations for "warm" plasma as an approximation to full "hot" plasma. Our approximation will be second-order in the Larmor radius, or first-order in $\lambda = \frac{k_x^2 v_{th}^2}{2\Omega^2}$. Retaining only terms up to $|n| = 2$ because the $|n| > 2$ terms have zeros of order > 1 at $\lambda = 0$ and thus give no contribution to a first-order approximation, this first-order approximation in λ of the dielectric tensor becomes

$$\epsilon = \epsilon_0 \left(1 + \sum_s (p_0 + p_1 + p_2)\right) \tag{10}$$

$$p_0 = \begin{bmatrix} 0 & 0 \\ 0 & \frac{e^{-\lambda}\omega_p^2\left(-2\lambda^2 I_0(\lambda) + 2\lambda^2 I_1(\lambda)\right)}{\omega^2\lambda} \end{bmatrix} \tag{11}$$

$$p_1 = \begin{bmatrix} -\frac{2e^{-\lambda}\omega_p^2 I_1(\lambda)}{\lambda(\omega^2-\Omega^2)} & -\frac{ie^{-\lambda}\omega_p^2\Omega(I_0(\lambda)-2I_1(\lambda)+I_2(\lambda))}{\omega(\omega^2-\Omega^2)} \\ \frac{ie^{-\lambda}\omega_p^2\Omega(I_0(\lambda)-2I_1(\lambda)+I_2(\lambda))}{\omega(\omega^2-\Omega^2)} & \frac{2e^{-\lambda}\omega_p^2\left(2\lambda^2 I_0(\lambda)-(1+2\lambda(1+\lambda))I_1(\lambda)\right)}{\lambda(\omega^2-\Omega^2)} \end{bmatrix} \tag{12}$$

$$p_2 = \begin{bmatrix} -\frac{8e^{-\lambda}\omega_p^2 I_2(\lambda)}{\lambda(\omega^2-4\Omega^2)} & -\frac{4ie^{-\lambda}\omega_p^2\Omega(I_1(\lambda)-2I_2(\lambda)+I_3(\lambda))}{\omega(\omega^2-4\Omega^2)} \\ \frac{4ie^{-\lambda}\omega_p^2\Omega(I_1(\lambda)-2I_2(\lambda)+I_3(\lambda))}{\omega(\omega^2-4\Omega^2)} & \frac{4e^{-\lambda}\omega_p^2\left(\lambda^2 I_1(\lambda)-(2+\lambda(2+\lambda))I_2(\lambda)\right)}{\lambda(\omega^2-4\Omega^2)} \end{bmatrix} \tag{13}$$

The symbols used are

- v_{th}: the thermal velocity
- k_x: wavenumber in the direction of propagation, assumed to be the x-direction
- $\lambda = \frac{k_x^2 v_{th}^2}{2\Omega^2}$: a second-order partial differential operator related to the Larmor radius, where ik_x corresponds to $\frac{\partial}{\partial x}$ in space.
- I_0, I_1, I_2, I_3 : modified Bessel functions of the first kind of order 0,1,2,3
- $\Omega = q|\vec{B}_0|/m$: cyclotron frequency for a particle specie of charge q and mass m
- $\omega_p = \sqrt{\frac{nq^2}{m\epsilon_0}}$: plasma frequency for a particle specie of charge q, mass m and density n

In the $\lambda \to 0$ limit, only p_1 is nonzero. We will approximate p_0 and p_2 to first-order in λ (i.e. $a + b\lambda$, where $a = 0$ for p_0 and p_2). To start, p_1 is approximated in the same way:

$$p_1 = p_{1,0} + p_{1,1}\lambda + O(\lambda^2) \tag{14}$$

However, this approximation is modified as follows

$$p_{1,\text{approx}} = p_{1,0} + (1 - p_{1,1}p_{1,0}^{-1}\lambda)^{-1} p_{1,1}\lambda \tag{15}$$

$p_{1,\text{approx}}$ is the simplest rational expression which at $\lambda = 0$ obeys

$$p_{1,\text{approx}} = p_1 \tag{16}$$

$$\frac{\partial}{\partial\lambda} p_{1,\text{approx}} = \frac{\partial}{\partial\lambda} p_1 \tag{17}$$

and, at $\lambda = \infty$

$$p_{1,\text{approx}} = p_1 = 0 \tag{18}$$

The approximation (15) is shown in figure 1 together with the exact expressions. The reason to use this approximation is based on stability considerations rather than approximation accuracy, see (29). These condiderations do not apply to p_0 and p_2. Nonetheless, one might attempt to construct rational expressions for p_0 and p_2 too. Let us stress that such expressions are not necessary to obtain second-order accuracy in v_{th}, and not sufficient to obtain third- or fourth-order accuracy in v_{th} (which would require truncating the summation at some $|n| > 2$). Improved expressions cannot be constructed using (15) : it requires the inverse of the zeroth-order term $p_{1,0}$, which is zero for p_0 and p_2. We can, however, use it to approximate p_0/λ and p_2/λ, and multiply the result once again by λ. For p_0 in particular, this amounts to constructing a Padé approximation at $\lambda = 0$ with first-order numerator and denominator. For both p_0 and p_2, the result has

a nonzero but finite limit at $\lambda \to \infty$. In what follows, we will mainly consider linear approximations for p_0 and p_2, and occasionally mention corresponding results for rational approximations.

We will assign three currents J_i $(i = 0, 1, 2)$ to every particle specie, of which the sum is the actual current associated with this specie. J_i will obey a constitutive equation producing (the first-order approximation of) p_i.

Starting with p_1

$$\vec{J}_1 = \epsilon_0 p_1 i\omega \vec{E} \tag{19}$$

$$(p_{1,\text{approx}} i\omega)^{-1} \vec{J}_1 = \epsilon_0 \vec{E} \tag{20}$$

which gives the surprisingly simple equation

$$i\omega \begin{bmatrix} (1+\lambda) & 0 \\ 0 & (1+3\lambda) \end{bmatrix} \begin{bmatrix} J_{1,x} \\ J_{1,y} \end{bmatrix} = \omega_p^2 \epsilon_0 \begin{bmatrix} E_x \\ E_y \end{bmatrix} - \begin{bmatrix} 0 & (1+2\lambda)\Omega \\ -(1+2\lambda)\Omega & 0 \end{bmatrix} \begin{bmatrix} J_{1,x} \\ J_{1,y} \end{bmatrix} \tag{21}$$

in a form analogous to (1), i.e. a derivative of a current as a function of the electric field and the current itself. This equation reduces to the cold plasma equations (i.e. to (1)) in the $\lambda \to 0$ limit.

p_0 and p_2 give rise to even simpler equations, but again with the same structure

$$i\omega \begin{bmatrix} J_{2,x} \\ J_{2,y} \end{bmatrix} = \omega_p^2 \epsilon_0 \lambda \begin{bmatrix} E_x \\ E_y \end{bmatrix} - \begin{bmatrix} 0 & 2\Omega \\ -2\Omega & 0 \end{bmatrix} \begin{bmatrix} J_{2,x} \\ J_{2,y} \end{bmatrix} \tag{22}$$

$$i\omega J_{0,y} = 2\omega_p^2 \epsilon_0 \lambda E_y \tag{23}$$

(there is no $J_{0,x}$). These currents do not get excited in the cold $\lambda \to 0$ limit.

If we had used rational approximations for p_0 and p_2 instead, these equations would be

$$\begin{bmatrix} i\omega(1+\lambda) & (2+3\lambda)\Omega \\ -(2+3\lambda)\Omega & i\omega(1+2\lambda) \end{bmatrix} \begin{bmatrix} J_{2,x} \\ J_{2,y} \end{bmatrix} = \epsilon_0 \omega_p^2 \lambda \begin{bmatrix} E_x \\ E_y \end{bmatrix} \tag{24}$$

$$i\omega \left(2+3\lambda\right) J_{0,y} = 4\epsilon_0 \omega_p^2 \lambda E_y \tag{25}$$

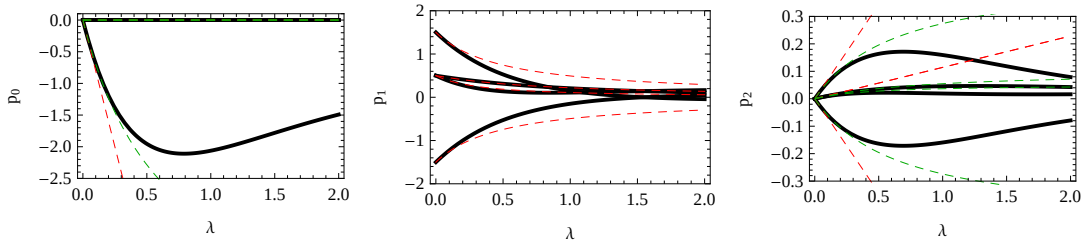

FIG. 1. Exact (solid black) and approximated (dashed red) matrix elements of p_i vs λ, for some arbitrarily-chosen parameters. The different way of approximating p_1 (see (15)) vs. p_0 and p_2 (1st-order Taylor series) is clearly visible. Dashed green are similar rational approximations for p_0 and p_2.

If we collect all fields in a single vector $V = [E_x, E_y, B_z, J_{2,x}, J_{2,y}, J_{1,x}, J_{1,y}, J_{0,y}]^T$, and replace $i\omega$ by $\frac{\partial}{\partial t}$ the resulting equations are

$$\frac{\partial}{\partial t} A_L V = A_R V \tag{26}$$

$$A_L = \begin{bmatrix} 1 & 0 & 0 & 0 & 0 & 0 & 0 & 0 \\ 0 & 1 & 0 & 0 & 0 & 0 & 0 & 0 \\ 0 & 0 & 1 & 0 & 0 & 0 & 0 & 0 \\ 0 & 0 & 0 & 1 & 0 & 0 & 0 & 0 \\ 0 & 0 & 0 & 0 & 1 & 0 & 0 & 0 \\ 0 & 0 & 0 & 0 & 0 & 1+\lambda & 0 & 0 \\ 0 & 0 & 0 & 0 & 0 & 0 & 1+3\lambda & 0 \\ 0 & 0 & 0 & 0 & 0 & 0 & 0 & 1 \end{bmatrix} \tag{27}$$

$$A_R = \begin{bmatrix} 0 & 0 & 0 & -1/\epsilon_0 & 0 & -1/\epsilon_0 & 0 & 0 \\ 0 & 0 & ik_x/(\epsilon_0\mu_0) & 0 & -1/\epsilon_0 & 0 & -1/\epsilon_0 & -1/\epsilon_0 \\ 0 & ik_x & 0 & 0 & 0 & 0 & 0 & 0 \\ \lambda\omega_p^2\epsilon_0 & 0 & 0 & 0 & -2\Omega & 0 & 0 & 0 \\ 0 & \lambda\omega_p^2\epsilon_0 & 0 & 2\Omega & 0 & 0 & 0 & 0 \\ \omega_p^2\epsilon_0 & 0 & 0 & 0 & 0 & 0 & -(1+2\lambda)\Omega & 0 \\ 0 & \omega_p^2\epsilon_0 & 0 & 0 & 0 & (1+2\lambda)\Omega & 0 & 0 \\ 0 & 2\lambda\omega_p^2\epsilon_0 & 0 & 0 & 0 & 0 & 0 & 0 \end{bmatrix} \tag{28}$$

A simple rescaling of the fields makes $A_L^{-1}A_R$ anti-hermitian, thereby proving unconditional stability of the continuous equations in uniform media. The proper rescaling is (29), which reduces, in the appropriate limit $\lambda \to 0$, to the rescaling for cold plasma derived in[1]. The very possibility of constructing this rescaling justifies the use of the approximation (15). Had we used a Taylor approximation, this rescaling would only have been possible at sufficiently small λ. The approximation (15) is a (possibly non-unique) answer to the question "In what way can we approximate p_1 to first-order accuracy in λ while ensuring that the eigenvalues of the resulting matrices remain purely imaginary?" A similar rescaling exists when using (24)-(25) instead of (22)-(23) : those, too, give rise to an unconditionally stable approximation. After this rescaling we get (30). Approximating $A_L^{-1}A_R$ (30) to second order in v_{th} (i.e. first order in λ) gives (31)

$$\begin{gathered} \vec{\mathcal{E}} = \sqrt{\epsilon_0}\vec{E} \qquad \vec{\mathcal{B}} = \frac{1}{\sqrt{\mu_0}}\vec{B} \qquad \vec{\mathcal{J}}_2 = \frac{i}{\omega_p\sqrt{\epsilon_0}\sqrt{\lambda}}\vec{J}_2 \\ \vec{\mathcal{J}}_{1,x} = \frac{\sqrt{1+\lambda}}{\omega_p\sqrt{\epsilon_0}}\vec{J}_{1,x} \quad \vec{\mathcal{J}}_{1,y} = \frac{\sqrt{1+3\lambda}}{\omega_p\sqrt{\epsilon_0}}\vec{J}_{1,y} \quad \vec{\mathcal{J}}_{0,y} = \frac{1}{\sqrt{2}\omega_p\sqrt{\epsilon_0}\sqrt{\lambda}}\vec{J}_{0,y} \end{gathered} \tag{29}$$

$$A_L^{-1}A_R = \begin{bmatrix} 0 & 0 & 0 & i\omega_p\sqrt{\lambda} & 0 & -\frac{\omega_p}{\sqrt{1+\lambda}} & 0 & 0 \\ 0 & 0 & ick_x & 0 & i\omega_p\sqrt{\lambda} & 0 & -\frac{\omega_p}{\sqrt{1+3\lambda}} & -\sqrt{2}\omega_p\sqrt{\lambda} \\ 0 & ick_x & 0 & 0 & 0 & 0 & 0 & 0 \\ i\omega_p\sqrt{\lambda} & 0 & 0 & 0 & -2\Omega & 0 & 0 & 0 \\ 0 & i\omega_p\sqrt{\lambda} & 0 & 2\Omega & 0 & 0 & 0 & 0 \\ \frac{\omega_p}{\sqrt{1+\lambda}} & 0 & 0 & 0 & 0 & 0 & -\frac{(1+2\lambda)\Omega}{\sqrt{1+\lambda}\sqrt{1+3\lambda}} & 0 \\ 0 & \frac{\omega_p}{\sqrt{1+3\lambda}} & 0 & 0 & 0 & \frac{(1+2\lambda)\Omega}{\sqrt{1+\lambda}\sqrt{1+3\lambda}} & 0 & 0 \\ 0 & \sqrt{2}\omega_p\sqrt{\lambda} & 0 & 0 & 0 & 0 & 0 & 0 \end{bmatrix} \tag{30}$$

$$A_L^{-1}A_R = \begin{bmatrix} 0 & 0 & 0 & \frac{ik_x v_{th}\omega_p}{\sqrt{2}\Omega} & 0 & -\omega_p + \frac{k_x^2 v_{th}^2 \omega_p}{4\Omega^2} & 0 & 0 \\ 0 & 0 & ick_x & 0 & \frac{ik_x v_{th}\omega_p}{\sqrt{2}\Omega} & 0 & -\omega_p + \frac{3k_x^2 v_{th}^2 \omega_p}{4\Omega^2} & \frac{ik_x v_{th}\omega_p}{\Omega} \\ 0 & ick_x & 0 & 0 & 0 & 0 & 0 & 0 \\ \frac{ik_x v_{th}\omega_p}{\sqrt{2}\Omega} & 0 & 0 & 0 & -2\Omega & 0 & 0 & 0 \\ 0 & \frac{ik_x v_{th}\omega_p}{\sqrt{2}\Omega} & 0 & 2\Omega & 0 & 0 & 0 & 0 \\ \omega_p - \frac{k_x^2 v_{th}^2 \omega_p}{4\Omega^2} & 0 & 0 & 0 & 0 & 0 & -\Omega & 0 \\ 0 & \omega_p - \frac{3k_x^2 v_{th}^2 \omega_p}{4\Omega^2} & 0 & 0 & 0 & \Omega & 0 & 0 \\ 0 & \frac{ik_x v_{th}\omega_p}{\Omega} & 0 & 0 & 0 & 0 & 0 & 0 \end{bmatrix} \tag{31}$$

Thus, the zeroth-order ($v_{th} = 0$, cold plasma) expression complemented with the first and second order finite temperature corrections to the time-domain equations of motion for perpendicular propagation are

$$\frac{\partial}{\partial t} V = A_L^{-1} A_R V \tag{32}$$

where $A_L^{-1} A_R$ is given by (31).

Here, we still assume all quantities are place-independent, as in the derivation of the dielectric tensor above. Later, we will generalize this equation to the place-dependent case.

The very existence of the rescaling (29) shows, of course, that the original non-rescaled equations (27)-(28) are themselves stable, and we do not need to use an extra Taylor approximation. A comparison of (27)-(28) and (31) is in order. Equations (27)-(28) result in a well-behaved lowest Bernstein root, even at exceedingly high λ. (31), on the other hand, suffers from an entirely non-physical Bernstein root deformation at high λ. It is possible to start from (31), construct a modified (21), and thus obtain the effective p_1 approximation for (31). This p_1 approximation differs from the constructed $p_{1,approx}$ (15). It still has the same value and derivative at $\lambda = 0$, but it has a nonzero (finite) limit at $\lambda \to \infty$.

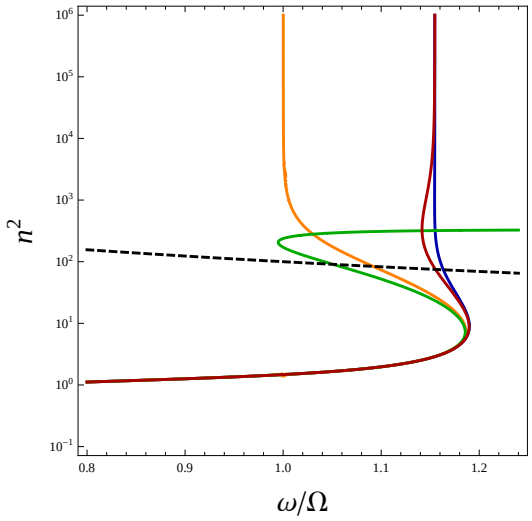

FIG. 2. Red : (27)-(28) result in a well-behaved if somewhat displaced lowest-order Bernstein root even at high λ. Green : (31) shows non-physical behaviour at high λ. Dark blue: based on the rational approximation of p_0 and p_2 (24)-(25). Orange : exact. Black dashed: $\lambda = 1$

The reader might wonder what happens in the general $k_\parallel \neq 0$ case. In that case, there are collisionless damping mechanisms[10,11]. Then we have to ensure that, at given real k, all ω are in the half-space corresponding to decaying or stable solutions (e.g. $\exp(i\omega t), \Im(\omega) \geq 0$). At present, this has proven problematic and we will stick to the $k_\parallel = 0$ case in this paper.

IV. EQUATIONS FOR PERPENDICULAR PROPAGATION IN NON-UNIFORM WARM PLASMA

In general, it is unclear how to generalize from a Fourier-spatial domain (k_x) expression, which assumes spatial uniformity, to the real-space (x) domain, when the plasma becomes non-uniform along x. To do so, we will ensure our expression (32) remains conservative (i.e. its eigenvalues are on the unit circle, as is to be expected in the absence of damping mechanisms), and let us guide by existing expressions for non-uniform warm plasma wave equations in the literature[3].

A wave equation may be obtained imediately by eliminating magnetic field and current degrees of freedom from

$$i\omega V = A_L^{-1} A_R V \tag{33}$$

Let

$$V = \begin{bmatrix} E \\ X \end{bmatrix} \tag{34}$$

where E are the electric degrees of freedom and X the to-be-eliminated magnetic and current degrees of freedom. For convenience, let us name the blocks of $A_L^{-1} A_R$

$$A_L^{-1} A_R = \begin{bmatrix} 0 & [XE] \\ [EX] & [XX] \end{bmatrix} \tag{35}$$

Then the wave equation becomes

$$i\omega E = [XE] \left(i\omega - [XX]\right)^{-1} [EX] E \tag{36}$$

Based on variational techniques, Colestock and Kashuba[3] derived a wave equation for non-uniform warm plasma which reduces to

$$\left(\frac{\partial}{\partial x} G \frac{\partial}{\partial x} + H \right) \cdot E = 0 \tag{37}$$

for perpendicular propagation (the additional term $F\frac{\partial}{\partial x}$ found in[3] drops out when $k_\parallel = 0$). Consider (28), and note that all correction terms are proportional to $\lambda \propto v_{th}^2$. There is not a single correction term proportional to v_{th}. For $k_\parallel = 0$, all corrections are second-order in the thermal velocity. This agrees with the result of[3], including the disappearing $F\frac{\partial}{\partial x}$ term and the fact that $G \propto v_{th}^2$ when $k_\parallel = 0$. Their result, being first-order in the Larmor radius, is not directly comparable to ours, given that there are no first-order corrections for perpendicular propagation. Nonetheless, we will let (37) guide us when choosing where to put spatial derivatives in the non-uniform generalisation of (31). This generalisation becomes

$$A_L^{-1}A_R = \begin{bmatrix} 0 & 0 & 0 & \delta_x\frac{v_{th}\omega_p}{\sqrt{2}\Omega} & 0 & -\omega_p-\delta_x^2\frac{v_{th}^2\omega_p}{4\Omega^2} & 0 & 0 \\ 0 & 0 & c\delta_x & 0 & \delta_x\frac{v_{th}\omega_p}{\sqrt{2}\Omega} & 0 & -\omega_p-\delta_x^2\frac{3v_{th}^2\omega_p}{4\Omega^2} & \delta_x\frac{v_{th}\omega_p}{\Omega} \\ 0 & c\delta_x & 0 & 0 & 0 & 0 & 0 & 0 \\ \frac{v_{th}\omega_p}{\sqrt{2}\Omega}\delta_x & 0 & 0 & 0 & -2\Omega & 0 & 0 & 0 \\ 0 & \frac{v_{th}\omega_p}{\sqrt{2}\Omega}\delta_x & 0 & 2\Omega & 0 & 0 & 0 & 0 \\ \omega_p+\frac{v_{th}^2\omega_p}{4\Omega^2}\delta_x^2 & 0 & 0 & 0 & 0 & 0 & -\Omega & 0 \\ 0 & \omega_p+\frac{3v_{th}^2\omega_p}{4\Omega^2}\delta_x^2 & 0 & 0 & 0 & \Omega & 0 & 0 \\ 0 & \frac{v_{th}\omega_p}{\Omega}\delta_x & 0 & 0 & 0 & 0 & 0 & 0 \end{bmatrix} \tag{38}$$

where $\delta_x = \frac{\partial}{\partial x}$ is the spatial derivative operator in the propagation direction. In (38), all quantities ω_p, Ω and v_{th} can be position-dependent.

V. A DISPERSION-RELATION-PRESERVING DISCRETISATION

We will discretize (38) using the techniques described in[1]. This involves constructing a discrete block-diagonal interpolator S_A, and a discrete "physics" matrix S_D (the discretized version of the operator $A_L^{-1}A_R$ from (38)), such that the space-discrete dispersion relation for $\frac{\partial}{\partial t}S_AV = S_DV$ equals the continuous dispersion relation except that the k_x from the continuous dispersion relation is replaced by its discrete tangent-version $\tan\left(k_x\frac{\Delta}{2}\right)\frac{2}{\Delta}$, where Δ is the space step (discretisation length) in the algorithm.

In section 3.3 of[1], stability was proved as follows: at every step, the equation $(S_A - S_D\Delta_t/2)V_+ = (S_A + S_D\Delta_t/2)V_-$ has to be solved, where V_- and V_+ represent the fields at this resp. the next time step. This is equivalent to $V_+ = (1 - S_A^{-1}S_D\Delta_t/2)^{-1}(1 + S_A^{-1}S_D\Delta_t/2)V_-$.

Suppose we have an eigenvector $\mathcal{V}$ of $S_A^{-1}S_D$ with eigenvalue κ

$$S_A^{-1}S_D\mathcal{V} = \kappa\mathcal{V} \tag{39}$$

then

$$(1 + S_A^{-1}S_D\Delta_t/2)\mathcal{V} = (1 + \kappa\Delta_t/2)\mathcal{V} \tag{40}$$

$$(1 - S_A^{-1}S_D\Delta_t/2)\mathcal{V} = (1 - \kappa\Delta_t/2)\mathcal{V} \tag{41}$$

$$(1 - S_A^{-1}S_D\Delta_t/2)^{-1}(1 + S_A^{-1}S_D\Delta_t/2)\mathcal{V} = \frac{1+\kappa\Delta_t/2}{1-\kappa\Delta_t/2}\mathcal{V} \tag{42}$$

thus, $\mathcal{V}$ is also an eigenvector of the time-stepping operator with eigenvalue $\frac{1+\kappa\Delta_t/2}{1-\kappa\Delta_t/2}$. If the eigenvalues κ are purely imaginary, the thus-obtained eigenvalues of the time-stepping operator all lie on the unit circle and the system is stable. Hence, it suffices to prove that the eigenvalues of $S_A^{-1}S_D$ are purely imaginary, which can be accomplished by finding a basis in which $S_A^{-1}S_D$ is skew-hermitian. In[1], we constructed S_A and S_D with periodic boundary conditions, and found that $S_A^{-1}S_D$ is skew-hermitian in the discrete Fourier-basis F (not to be confused with the previously-mentioned k_x spatial Fourier-domain)

$$F_{j,k} = \frac{1}{\sqrt{n}}\exp\left(\frac{-2\pi i}{n}(j-1)(k-1)\right) \tag{43}$$

$$M_F = FS_A^{-1}S_DF^{-1} \tag{44}$$

$$M_F^\dagger = -M_F \tag{45}$$

where n is the amount of discretisation points, assumed odd.

In order for this approach to work for the warm plasma model (38), we need to modify our interpolators to avoid running into commutation issues.

Consider $A_L^{-1}A_R$ (38), from which we will construct S_D. Let us focus on the discretized counterparts of (46), i.e. elements $(1,6)$ and $(6,1)$:

$$\begin{matrix} -\omega_p-\delta_x^2\frac{v_{th}^2\omega_p}{4\Omega^2} & (1,6) \\ \omega_p+\frac{v_{th}^2\omega_p}{4\Omega^2}\delta_x^2 & (6,1) \end{matrix} \tag{46}$$

Discretisation according to the techniques of[1] gives

$$\begin{matrix} -M_i^2\omega_p - M_d^2\frac{v_{th}^2\omega_p}{4\Omega^2} & (1,6) \\ M_i^2\omega_p+\frac{v_{th}^2\omega_p}{4\Omega^2}M_d^2 & (6,1) \end{matrix} \tag{47}$$

where the discrete interpolation matrix and the discrete derivative matrix are

$$M_i = \frac{1}{2}\begin{pmatrix} 1 & 1 & 0 & 0 & 0 & \dots \\ 0 & 1 & 1 & 0 & 0 & \dots \\ & & \vdots & & & \ddots \\ 1 & 0 & 0 & \dots & 0 & 1 \end{pmatrix} \tag{48}$$

$$M_d = \frac{1}{\Delta}\begin{pmatrix} 1 & -1 & 0 & 0 & 0 & \dots \\ 0 & 1 & -1 & 0 & 0 & \dots \\ & & \vdots & & & \ddots \\ -1 & 0 & 0 & \dots & 0 & 1 \end{pmatrix} \tag{49}$$

and the *position-dependent* quantities ω_p and $\frac{v_{th}^2\omega_p}{4\Omega^2}$ become diagonal matrices with diagonal element (i,i) representing the position-dependent quantity at the ith discretisation point.

The corresponsing blocks $(1,1)$ and $(6,6)$ of S_A are both M_i^2, thus, the corresponding elements of $S_A^{-1}S_D$ become

$$\begin{matrix} -\omega_p - M_i^{-2}M_d^2\frac{v_{th}^2\omega_p}{4\Omega^2} & (1,6) \\ \omega_p + M_i^{-2}\frac{v_{th}^2\omega_p}{4\Omega^2}M_d^2 & (6,1) \end{matrix} \tag{50}$$

Because M_i^{-2} does not in general commute with $\frac{v_{th}^2\omega_p}{4\Omega^2}$, the resulting matrix is not skew-hermitian in the Fourier basis. However, this can be remedied: suppose we introduce a modified interpolator $\mathcal{M}_i$ and force it to obey the commutation relation $\mathcal{M}_i^{-2}\frac{v_{th}^2\omega_p}{4\Omega^2} = \frac{v_{th}^2\omega_p}{4\Omega^2}M_i^{-2}$. We introduce this modified interpolator in $(6,1)$ while leaving $(1,6)$ as is

$$\begin{matrix} -M_i^2\omega_p - M_d^2\frac{v_{th}^2\omega_p}{4\Omega^2} & (1,6) \\ \mathcal{M}_i^2\omega_p + \frac{v_{th}^2\omega_p}{4\Omega^2}M_d^2 & (6,1) \end{matrix} \tag{51}$$

Element $(1,1)$ of S_A remains M_i^2 but element $(6,6)$ is replaced by $\mathcal{M}_i^2$. If we multiply (51) by S_A^{-1} we now get

$$\begin{matrix} -\omega_p - M_i^{-2}M_d^2\frac{v_{th}^2\omega_p}{4\Omega^2} & (1,6) \\ \omega_p + \frac{v_{th}^2\omega_p}{4\Omega^2}M_i^{-2}M_d^2 & (6,1) \end{matrix} \tag{52}$$

which is properly skew-hermitian in the Fourier basis, as we will now show. Let F be the discrete Fourier transform matrix, whose inverse is its conjugate transpose $F^{-1} = F^\dagger$. The first terms of $(1,6)$ and $(6,1)$ in (52) require (53)-(56) and the second terms lead to (57)-(60)

$$(F\omega_pF^{-1})^\dagger = -(-F\omega_pF^\dagger) \tag{53}$$
$$(F\omega_pF^\dagger)^\dagger = -(-F\omega_pF^\dagger) \tag{54}$$
$$(F^\dagger)^\dagger\omega_p^\dagger F^\dagger = -(-F\omega_pF^\dagger) \tag{55}$$
$$F\omega_pF^\dagger = -(-F\omega_pF^\dagger) \tag{56}$$
$$(F\frac{v_{th}^2\omega_p}{4\Omega^2}F^\dagger FM_i^{-2}M_d^2F^\dagger)^\dagger = -(-FM_i^{-2}M_d^2F^\dagger F\frac{v_{th}^2\omega_p}{4\Omega^2}F^\dagger) \tag{57}$$
$$(FM_i^{-2}M_d^2F^\dagger)^\dagger(F\frac{v_{th}^2\omega_p}{4\Omega^2}F^\dagger)^\dagger = -(-FM_i^{-2}M_d^2F^\dagger F\frac{v_{th}^2\omega_p}{4\Omega^2}F^\dagger) \tag{58}$$
$$FM_i^{-2}M_d^2F^\dagger((F^\dagger)^\dagger\left(\frac{v_{th}^2\omega_p}{4\Omega^2}\right)^\dagger F^\dagger) = -(-FM_i^{-2}M_d^2F^\dagger F\frac{v_{th}^2\omega_p}{4\Omega^2}F^\dagger) \tag{59}$$
$$FM_i^{-2}M_d^2F^\dagger F\frac{v_{th}^2\omega_p}{4\Omega^2}F^\dagger = -(-FM_i^{-2}M_d^2F^\dagger F\frac{v_{th}^2\omega_p}{4\Omega^2}F^\dagger) \tag{60}$$
$$FM_i^{-2}M_d^2F^\dagger = \mathrm{diag}\left(0, \frac{i}{2}\tan\left(\frac{\pi}{n}\right), \frac{i}{2}\tan\left(\frac{2\pi}{n}\right), \ldots, \frac{i}{2}\tan\left(\frac{(n-1)\pi}{n}\right)\right)^2 \tag{61}$$

Use was made of the fact that $FM_i^{-2}M_d^2F^\dagger$, ω_p and $\frac{v_{th}^2\omega_p}{4\Omega^2}$ are both diagonal and purely real. For $FM_i^{-2}M_d^2F^\dagger$, an explicit formula is given in (61) where n is the size of the interpolator and differentiator matrices, i.e. the number of discretisation points. For details see[1].

It is only required to use such a modified interpolator when we have derivative operators on the right side of the expressions, i.e. only the constitutive equations for the currents need these modified interpolators. For every constitutive equation, it is possible to construct such a modified interpolator to ensure $S_A^{-1}S_D$ remains skew-hermitian (and thus the resulting set of equations remains stable). The matrices describing the position-dependent background quantities are diagonal thus these modified interpolators may be determined efficiently.

While this discretisation retains much of the favourable properties described in[1], there is one property in particular which it does not retain: for cold plasma, it was possible to construct a sparse Schur complement to ensure the size of the to-be-solved set of equations is independent of the number of species. The presence of spatial derivative operators in the constitutive equations (there are no such operators in the cold plasma equations of motion) makes that optimisation procedure no longer viable. The discrete current-current interaction matrix now contains interpolators, it is no longer purely local and thus not trivially invertible. However: note that, entirely in the spirit of[1], second-order differentiators were paired with second-order interpolators. The finite-difference second-order differentiator is naturally collocated with the original grid (as opposed to the first-order differentiator, whose result exists on points located in between original grid-points). One might then won-

der: why use the second-order interpolator at all? At least in the uniform case, it appears the system remains stable when we replace the second-order interpolator M_i^2 by the appropriate unit matrix, in which case the optimizations of[1] remain applicable.

VI. NUMERICAL EXAMPLE

A. Dispersion relation for the uniform case

We numerically determined the dispersion relation in the electron cyclotron range[9], showing the lowest-order Bernstein wave (figure 3). As expected, the eigenvalues of the time-stepping operator $(S_A - S_D\Delta_t/2)^{-1}(S_A + S_D\Delta_t/2)$ with periodic boundary conditions all lie on the unit circle, even for solutions which violate the $\lambda \ll 1$ condition. We used the same parameters as[9], i.e. a single-specie (electron) plasma with $(\omega_p/\Omega)^2 = 1/2, \beta = (\omega_p/\Omega)^2(v_{th}/c)^2 = 1/100$. The simulation used 301 discretisation points, corresponding to 2408×2408 S_A and S_D matrices. The quantity plotted in figure 3 is $n^2 = (kc/\omega)^2$. Note that $\lambda = n^2(\omega/\Omega)^2\beta$, which enables us to plot constant-λ curves, separating areas where the approximation is good (small λ) from those where the approximation is bad (high λ). The numerical results are represented by red dots for $n^2 > 0$, which were calculated using numerically-determined eigenvectors of the time-stepping operator with periodic boundary conditions, a procedure which produces all solutions at once but can only give propagating ($n^2 > 0$) solutions. Therefore, additional $n^2 < 0$ solutions (red squares) were calculated using different boundary conditions : (the fields at the left of the simulation region)=(the fields at the right of the simulation region)$\times \exp(-k_i L)$, where k_i is the desired imaginary part of k and L is the length of the simulation region. Using this boundary condition, the eigenvectors of the time-stepping operator become complex exponentials with given k_i, and the evanescent $n^2 < 0$ solutions can be found among them.

We then tested the same configuration by time-stepping (as is the point of a time-domain algorithm) in figure 4. The source frequency was $\omega/\Omega = 1.05$. Indeed, the slowly-propagating short-wavelength Bernstein wave becomes apparent.

B. A non-uniform example

If the plasma temperature (v_{th} or $\beta = (\omega_p/\Omega)^2(v_{th}/c)^2$) varies with position, the wavelength of the Bernstein wave will also change. In figure 5, we show β varying with position. The corresponding dispersion relation is shown in figure 6. The system also remains stable in this non-uniform case as can be seen from the eigenvalues of the time-stepping operator in figure 7. Finaly, the $\mathcal{E}_x$ component is shown in figure 8.

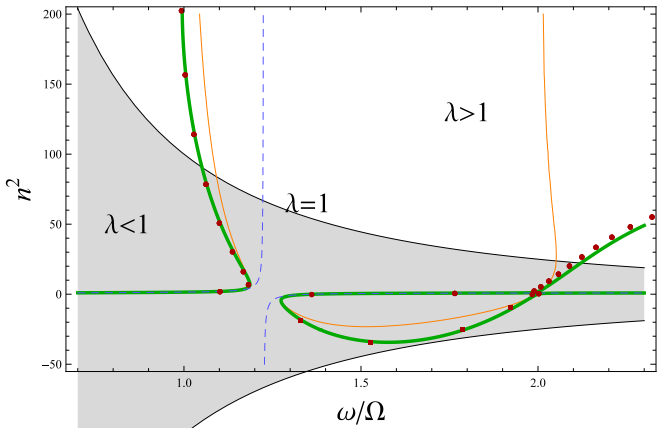

FIG. 3. $n^2 = (kc/\omega)^2$ vs ω/Ω. Dashed blue: cold plasma behaviour. Orange: actual hot plasma behaviour. Green: warm dispersion relation in the electron cyclotron frequency range. Black : $\lambda = 1$ (not a constant on the graph because n is plotted instead of k, the approximation is good when λ is small). Red dots : numerically obtained dispersion relation. See also figure 27.2 in[9]

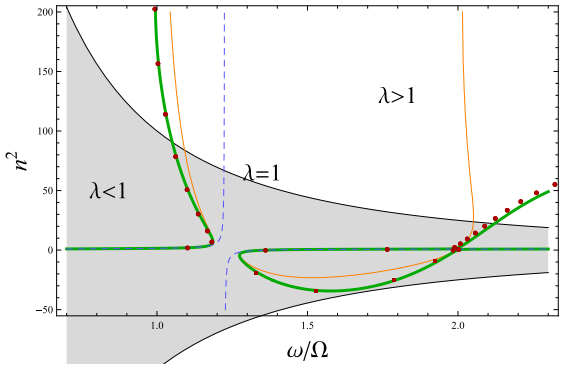

FIG. 4. Configuration of figure 3 (with 1801 discretisation points) in time. The source is at $x = 0$ and the boundary conditions are periodic. The fast-propagating long-wavelength cold root first becomes apparent, and later the much shorter-wavelength Bernstein root also appears.

As expected from the other figures, the wavelength is shorter when β is lower.

VII. CONCLUSION

In this paper, we derived finite-temperature corrections to the equations of motion for perpendicular propagation in magnetized plasma, essentially by transforming a finite-order approximation of the hot plasma dielectric tensor back to time-domain. We have shown that the resulting equations may be successfully discretized using the techniques described in[1]. It is true that the $k_\parallel = 0$ case is rather restrictive : interesting collisionless absorption mechanisms only show up in the $k_\parallel \neq 0$

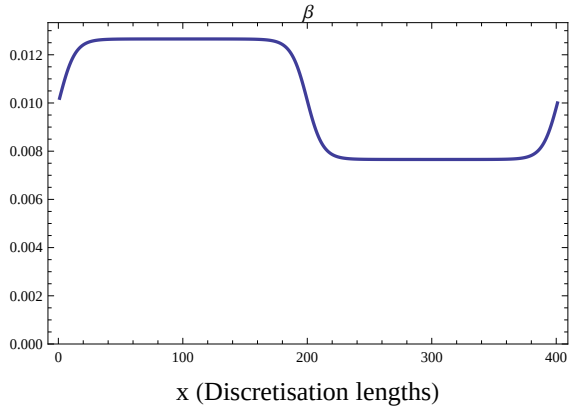

FIG. 5. $\beta = (\omega_p/\Omega)^2(v_{th}/c)^2$ vs. position for a non-uniform example.

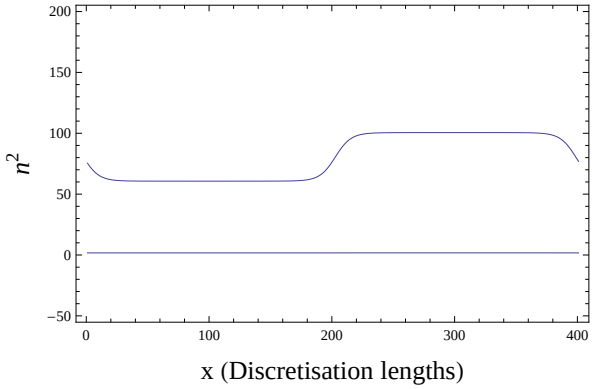

FIG. 6. Corresponding space-dependent dispersion relation showing the long-wavelength cold root and the strongly β-dependent Bernstein root.

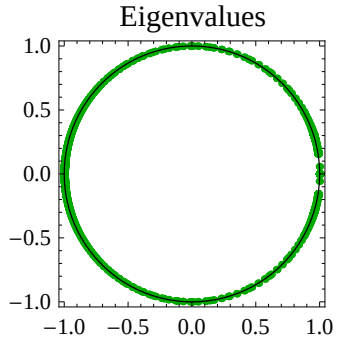

FIG. 7. The eigenvalues are on the unit circle in the non-uniform case. The system is stable.

case. However, this work shows that at least some of the more complicated behaviour of plasmas can be modeled in time-domain without having to resort to particle-in-cell techniques or explicit use of the Vlasov equation.

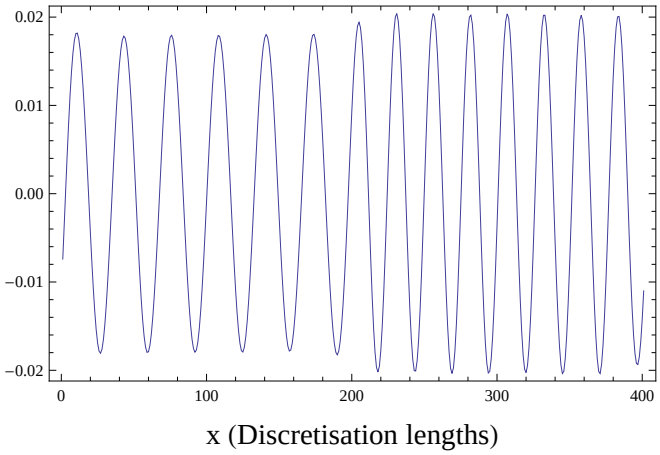

FIG. 8. $\mathcal{E}_x$ vs. position.

[1] W. Tierens and D. D. Zutter, "An unconditionally stable time-domain discretization on cartesian meshes for the simulation of nonuniform magnetized cold plasma," Journal of Computational Physics (2012).
[2] H. P. Laqua, "Electron bernstein wave heating and diagnostic," Plasma Physics and Controlled Fusion **49** (2007).
[3] P. Colestock and R. Kashuba, "The theory of mode conversion and wave damping near the ion cyclotron frequency," Nuclear fusion **23** (1983).
[4] D. V. Eester and R. Koch, "A variational principle for studying fast-wave mode conversion," Plasma Physics and Controlled Fusion **40** (1998).
[5] J. Young, "A full finite difference time domain implementation for radio wave propagation in a plasma," Radio science (1994).
[6] D. N. Smithe, "Time domain modeling of plasmas at RF time-scales," Journal of Physics: Conference Series **78** (2007).
[7] D. N. Smithe, "Finite-difference time-domain simulation of fusion plasmas at radiofrequency time scales," Physics of Plasmas **14**, 2537–2549 (2007).
[8] R. M. Joseph, S. C. Hagness, and A. Taflove, "Direct time integration of Maxwell's equations in linear dispersive media with absorption for scattering and propagation of femtosecond electromagnetic pulses," Optics Letters (1991).
[9] M. Brambilla, *Kinetic theory of plasma waves* (Clarendon Press, 1998).
[10] R. Bilato and M. Brambilla, "On the nature of "collisionless" Landau damping," Communications in Nonlinear Science and Numerical Simulation **13**, 18 – 23 (2008).
[11] T. Zhou, Y. Gue, and C. Shu, "Numerical study on Landau damping," Physica D , 322 – 333 (2001).